Applied Energy 221 (2018) 450–463

Contents lists available at ScienceDirect

Applied Energy

journal homepage: www.elsevier.com/locate/apenergy

An autonomous hierarchical control for improving indoor comfort and energy efficiency of a direct expansion air conditioning system

Jun Mei[a,*], Xiaohua Xia[a], Mengjie Song[b]

[a] Centre of New Energy Systems, Department of Electrical, Electronic and Computer Engineering, University of Pretoria, Pretoria 0028, South Africa
[b] Energy Research Institute at NTU (ERI@N), Research Techno Plaza, Nanyang Technological University, 50 Nanyang Drive, Singapore 637553, Singapore

HIGHLIGHTS

- We propose a novelty control strategy to save more energy consumed and cost.
- The results validate the proposed method for improving comfort levels.
- The proposed hierarchical control method is easy to implement in practice.
- Performance of designed control strategy is better than the previous strategies.
- The designed control method is not very sensitive to the system parameters.

ARTICLE INFO

Keywords:
Autonomous hierarchical control
PMV index
Model predictive control
Energy saving
time-of-use

ABSTRACT

This paper presents an autonomous hierarchical control method for a direct expansion air conditioning system. The control objective is to maintain both thermal comfort and indoor air quality at required levels while reducing energy consumption and cost. This control method consists of two layers. The upper layer is an open loop controller that allows obtaining tradeoff steady states by optimizing the energy cost of the direct expansion air conditioning system and the value of predicted mean vote under the time-of-use price structure of electricity. On the other hand, the lower layer designs a model predictive controller, which is in charge of tracking the tradeoff steady states calculated by the upper layer. Control performance of the proposed control method is compared to a conventional control strategy. The results show that the proposed control strategy reduces the energy consumption and energy cost of the direct expansion air conditioning system by 31.38% and 33.85%, respectively, while maintaining both the thermal comfort and indoor air quality within acceptable ranges, which validate the proposed methodology in terms of both comfort and energy efficiency.

1. Introduction

It is well known that the building sector is responsible for almost 40% of the global total energy consumption, costing $350 billion per year. Since energy management of building air conditioning (A/C) systems is a key factor in improving the energy efficiency and reducing the energy cost of buildings, optimal control of the A/C systems has increasingly attracted research attention. Energy efficiency improvement of buildings can also be performed at different levels of time scale and building subsystems such as ambient intelligence [1–3], energy balance [4–8], building portfolio management and planning [9–14] and energy-water nexus [15,16].

Since people spend much time indoors, thermal comfort and indoor air quality (IAQ) are important issues in A/C control. Thermal comfort has been accomplished by regulating temperature and relative humidity of indoor air. In view of air quality, CO_2 concentration is used as an indicator because carbon dioxide is the main fluid waste from occupants in a building. The indoor air temperature, humidity and CO_2 concentration are affected by A/C systems, lighting, the number of occupants and natural ventilation. They are also affected by outdoor environment, including the outside temperature, humidity, CO_2 concentration and solar irradiation. The A/C system needs to provide a comfortable environment for occupants with the minimum energy consumption and cost. There are strong interactions of energy cost and energy consumption with thermal comfort and IAQ. This crucial fact has been recognised by industrial and academic researchers.

Researchers proposed various control strategies to improve energy efficiency and comfort temperature [17–20]. In [21], the authors

* Corresponding author.
E-mail address: junmei027@gmail.com (J. Mei).

https://doi.org/10.1016/j.apenergy.2018.03.162
Received 29 January 2018; Received in revised form 15 March 2018; Accepted 30 March 2018

Nomenclature

A_1	heat transfer area of the DX evaporator in the dry-cooling region, m^2
A_2	heat transfer area of the DX evaporator in the wet-cooling region, m^2
A_0	total heat transfer area of the DX evaporator, m^2
A_{win}	total window area, m^2
C_c	CO_2 concentration of conditioning space, ppm
C_s	CO_2 concentration of supply air, ppm
C_z	specific heat of air, kJ kg^{-1} °C^{-1}
G	amount of CO_2 emission rate of people, m^3/s
h_{fg}	latent heat of vaporization of water, kJ/kg
h_{r1}	enthalpy of refrigerant at evaporator inlet, kJ/kg
h_{r2}	enthalpy of refrigerant at evaporator outlet, kJ/kg
k_{spl}	coefficient of supply fan heat gain, kJ/m^3
k_P,k_I	proportional and integral gains of PI controller
m_r	mass flow rate of refrigerant, kg/s
M_{load}	moisture load of conditioned space, kg/s
$Occp$	number of occupants
Q_{load}	sensible heat load of conditioned space, kW
Q_{rad}	solar radiative heat flux density, W/m^2
Q_{spl}	heat gain of supply fan, kW
T_d	air temperature leaving the dry-cooling region on air side, °C
T_s	temperature of supply air from the DX evaporator, °C
T_w	temperature of the DX evaporator wall, °C
T_z	air temperature of conditioned space, °C
T_0	temperature of outside, °C
v_a	air face velocity for DX cooling coil, m/s
v_f	air volumetric flow rate, m^3/s
V	volume of conditioned space, m^3
V_{h1}	air side volume of the DX evaporator in the dry-cooling region on air side, m^3
V_{h2}	air side volume of the DX evaporator in the wet-cooling region on air side, m^3
W_s	moisture content of supply air from the DX evaporator, kg/kg dry air
W_z	air moisture content of conditioned space, kg/kg dry air
W_0	air moisture content of outside, kg/kg dry air
α_1	heat transfer coefficient between air and the DX evaporator wall in the dry-cooling region, kW m^{-2} °C^{-1}
α_2	heat transfer coefficient between air and the DX evaporator wall in the wet-cooling region, kW m^{-2} °C^{-1}
ε_{win}	transmissivity of glass of window
ρ	density of moist air, kg/m^3

proposed an optimization method on room air temperature to improve both thermal comfort and energy efficiency. In [22], Cigler et al. presented an MPC to minimize the energy consumption and the value of predicted mean vote (PMV) index simultaneously. The simulation results showed that it would save 10–15% energy while keeping the comfort temperature within a level defined by standards. A hierarchical control method was proposed to improve the energy efficiency while maintaining the indoor temperature equal to a value such that the PMV index will be equal to zero reported in [23]. The results showed that it would reduce more energy consumption in comparison with previous work [24]. An economic model predictive control (MPC) method for optimising the building demand and energy cost under a TOU price policy under given bounded comfort temperature is studied in [25]. It demonstrated that this strategy is capable of reducing more energy cost and shifting the peak demand to off-peak hours while keeping the temperature at comfort bounded. In [26,27], the authors presented an MPC that minimises the expected energy cost and bounds of temperature comfort violations. One can note that all the above contributions focus on improving the energy efficiency of buildings by heating, ventilation and air conditioning (HVAC) temperature control. However, ensuring the indoor humidity at an appropriate level is also a crucial problem since it directly affects building occupants' thermal comfort and the operating efficiency of building A/C installations [28]. In fact, in cities with high humid climates, such as Cape Town or Hongkong, high humidity may still adversely impact indoor thermal comfort level and energy efficiency of building A/C systems even when indoor air temperature has been maintained at a desired value.

In recent years, a model-based predictive control algorithm proposed for HVAC system to control indoor temperature and humidity simultaneously taking into account energy efficiency was reported in [29]. In the study, the indoor air temperature and humidity are considered in two separate control loops. However, the control method remained inadequate fundamentally. A multi-input-multi-output (MIMO) control strategy is proposed for controlling the indoor air temperature and humidity simultaneously by varying the speeds of the compressor and the supply fan in an experimental direct expansion (DX) A/C system in [30]. In the research, the authors considered the coupling effect between indoor air temperature and humidity; so that the control accuracy and sensitivity can be improved. However, the control strategy was carried out based on the linearized system around a particular operational point, i.e., fixing the supply air temperature and moisture content. For a DX A/C system, its inlet air temperature and humidity affect its output cooling capacity directly [31]. The development of a physical model-based controller for a variable speed DX A/C system, aiming at controlling indoor air temperature and humidity simultaneously should be within its entire possible working range. An artificial neural network (ANN)-based modeling and control for an experimental variable speed DX A/C system was proposed to control the indoor air temperature and humidity simultaneously [32]. A real-time neural inverse optimal control for the simultaneous control of indoor air temperature and humidity using a DX A/C system was reported in [33]. A three-evaporator air conditioning system for simultaneous indoor air temperature and humidity control was studied in [34]. In [35], a fuzzy logic controller was developed for temperature and humidity control. The results demonstrated that the fuzzy logic controller developed can achieve the simultaneous control over indoor air temperature and humidity, with a reasonable control accuracy and sensitivity.

Nowadays, the indoor air quality (IAQ) is also an important issue for users, especially in office buildings, since a poor IAQ has a direct effect on work efficiency. In [36,37], Zhu et. al., studied indoor air temperature, humidity and CO_2 concentration control simultaneously without considering their coupling effects. However, these coupling effects cannot be ignored in many cases. In fact, the experimental investigation [38] suggested that the indoor CO_2 concentration affected indoor air temperature. Furthermore, indoor humidity was correlated with CO_2 concentration according to measurement results reported in [39]. Indoor air temperature, relative humidity and CO_2 levels assessment in academic buildings with different HVAC systems was studied in [40]. In [41], this study aimed to establish an optimal occupant behavior that can reduce total energy consumption and improve the thermal comfort, IAQ and visual comfort simultaneously by an energy simulation and optimization tool. In [42], an energy-optimised open loop controller and a closed-loop regulation of the multi-input-multi-output (MIMO) MPC schemes for a DX A/C system were proposed to improve both thermal comfort and IAQ, while minimizing energy consumption. The results showed that the energy savings were achieved and thermal comfort and IAQ were improved. However, the setpoints of thermostats

are constant over a 24-h period. This strategy is simple but not optimal in the sense of energy efficiency or cost-effectiveness. On the other hand, the outside temperature and humidity are also constant over a 24-h period in the study, while the outdoor air temperature and humidity vary over a 24-h period actually. Besides, a ventilation fan with an independent pressure swing absorption box was added to improve IAQ, which would increase the complexity and the cost of hardware.

Reduction of energy consumption and cost is important to promote economic and environmental development. Therefore, it is of great interest to develop advanced control technologies for building A/C systems to reduce energy consumption and cost. However, several control methods were proposed recently to reduce energy consumption and cost of building A/C systems while maintaining thermal comfort and IAQ at required levels. In this paper, an autonomous hierarchical control method is proposed to ensure occupants' thermal comfort and IAQ in a certain environment, and at the same time, tries to reduce the energy consumption and cost for a DX A/C system. The use of the DX A/C system has many advantages. When compared to central chilled water-based A/C systems, DX A/C systems are simpler in system configuration, more energy efficient [43] and cost less to own and maintain. Therefore, DX A/C systems have been widely used over recent decades in buildings, especially in small to medium scaled buildings. The proposed control strategy will further enhance the performance of DX A/C system. The proposed autonomous hierarchical controller is formed by two layers. (i) The upper layer consists of a nonlinear optimizer, which provides trajectory references of indoor air temperature, humidity and CO_2 concentration within acceptable ranges. This controller uses an open loop controller to optimise the energy cost of the DX A/C system and the value of the PMV index under a TOU price policy. (ii) Meanwhile, the lower layer contains a closed-loop MPC controller to track adaptively and automatically the trajectory references of indoor air temperature, humidity and CO_2 concentration calculated by the upper layer. To demonstrate the advantage of the proposed control method, we will compare the proposed control and a baseline control strategy.

The contributions of this paper are listed below. The references of indoor air temperature, humidity and CO_2 concentration are not needed. We present a method to autonomously and adaptively optimise and generate all steady states on required levels of thermal comfort and IAQ which could vary during the day. The volume of outside air entering into the system is fixed in [37,42]. In our study, the volumes of fresh air entering the DX A/C system are considered to vary with the environment over a 24-h period and are optimised by the proposed method. Moreover, a supply fan to drive the pressure swing absorption with a built-in PI controller is proposed to reduce indoor CO_2 concentration in this paper. Hence, it has the potential of reducing the complexity of computation and the cost of hardware. The PMV index is traditionally used as an indicator of indoor thermal comfort. In this study, it is used as an indicator of thermal comfort and that of IAQ when the indoor air CO_2 concentration is at its steady state.

The remainder of this paper includes five parts. The nonlinear reduced order dynamical system models, the energy consumption models of the DX A/C system and the indoor cooling load models are presented in Section 2. The proposed control method is presented in Section 3. Results are given in Section 4, and conclusions are drawn in Section 5.

2. System model

2.1. DX A/C system

A DX A/C system is mainly composed of two parts, which are the DX refrigeration plant (refrigerant side) and air-distribution sub-system (air side). Fig. 1 is the simplified schematic diagram of the DX A/C system. The DX refrigeration side mainly consists of the following components: a variable speed rotor compressor, an electronic expansion valve (EEV), a high-efficiency tube-louver-finned DX evaporator and an air-cooled tube-plant-finned condenser. The evaporator is placed inside the supply air duct on the air side to work as a DX air cooling coil which is located in the room. The air side includes an air-distribution ductwork with return air dampers, a variable speed centrifugal supply fan, a pressure swing absorption (PSA) box, a conditioned space and a damper position which is used to control the proportion of return air to outside air. The PSA box absorbs the CO_2 contaminant concentration to maintain IAQ. The allowed fresh air is also used to improve indoor fresh air ratio.

2.2. DX A/C models

The dynamic model of the DX A/C system is mainly derived from the principles of energy and mass balance. The model is highly nonlinear with respect to temperature, moisture content and CO_2

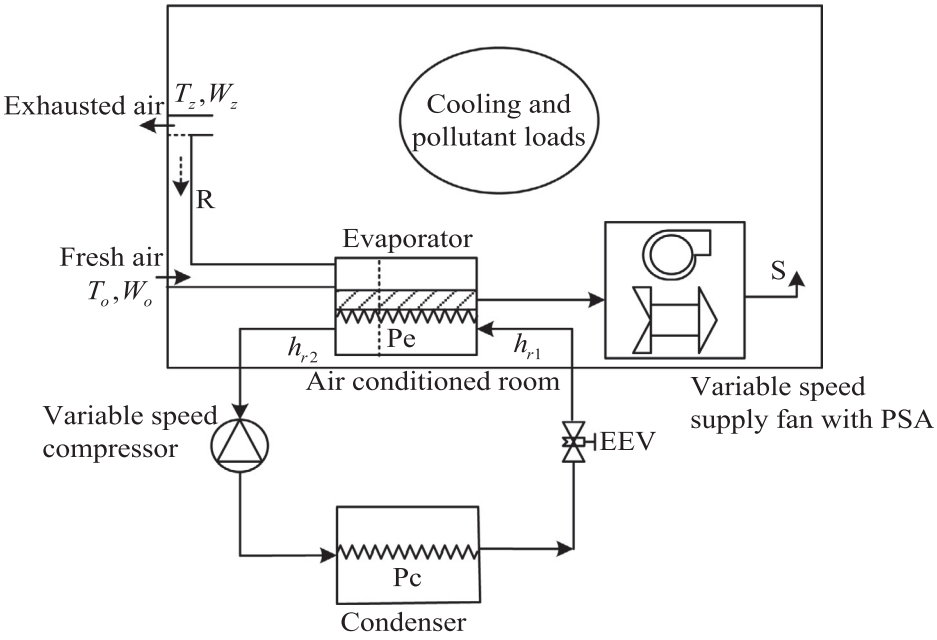

Fig. 1. Simplified diagram of DX air conditioning system.

concentration. In this paper, the system is assumed to operate in the cooling mode. The basic operation and assumptions of the system on the cooling mode are given for the purpose of simplicity as below: (i) It is assumed that p% of outside air enters into the system and gets mixed with (100−p)% of recirculated air entering into the system. (ii) Sufficient air mixing occurs inside the heat exchangers where the air gets conditioned. (iii) Two regions on the air side of the DX evaporator are shown in Fig. 2, i.e., dry-cooling region (sensible heat transfer only) and wet-cooling region (sensible and latent heat transfer region). The coupling between both regions that the outlet air properties of the first one (dry-cooling region) are the inlet air conditions entering the wet-cooling region. Therefore, the area from zero to A_1 pertains to the dry-cooling region and the rest of the total surface area is the wet-cooling region A_2. The boundary between the dry surface and the wet surface within a DX evaporator can be determined by the distribution of the surface temperature. It is a time-varying parameter under different conditions. (iv) Thermal losses in air ducts are neglected. (v) The supply air enters into the air-conditioned space to offset the cooling and pollutant loads acting upon the system. (vi) The air in the conditioned room exhausts through a fan, where (100−p)% of the air is recirculated and the rest is exhausted from the system through the fan.

Based on the above assumptions, the dynamic mathematical model for the DX A/C system for controlling indoor air temperature, moisture content and CO_2 concentration is developed based on the energy and mass conservation principles, which can be described by the following equations:

$$C_z\rho V\frac{dT_z}{dt} = C_z\rho v_f(T_s-T_z) + Q_{load}, \tag{1}$$

$$\rho V\frac{dW_z}{dt} = \rho v_f(W_s-W_z) + M_{load}, \tag{2}$$

$$C_z\rho V_{h1}\frac{dT_d}{dt} = C_z\rho v_f((1-p\%)T_z + p\%T_0-T_d) + \alpha_1 A_1\left(T_w-\frac{(1-p\%)T_z + p\%T_0 + T_d}{2}\right), \tag{3}$$

$$C_z\rho V_{h2}\frac{dT_s}{dt} + \rho V_{h2}h_{fg}\frac{dW_s}{dt} = C_z\rho v_f(T_d-T_s) + h_{fg}\rho v_f((1-p\%)W_z + p\%W_0-W_s) + \alpha_2 A_2\left(T_w-\frac{T_d + T_s}{2}\right), \tag{4}$$

$$C_w\rho_w V_w\frac{dT_w}{dt} = \alpha_1 A_1\left(\frac{(1-p\%)T_z + p\%T_0 + T_d}{2}-T_w\right) + \alpha_2 A_2\left(\frac{T_d + T_s}{2}-T_w\right) -(h_{r2}-h_{r1})m_r, \tag{5}$$

$$V\frac{dC_c}{dt} = v_s(C_s-C_c) + C_{load}. \tag{6}$$

More details for the system models (1)–(6) can be found in [42,44]. Note that the system models (1)–(5) without outside air entering into the system have been reported and validated by the experimental demonstrated in [44]. The model (6) has been verified in [45] by using an online learning and estimation approach for model parameter identification with acceptable accuracy.

We assume that the CO_2 concentration absorption rate v_s is a PI controller designed by

$$v_s = k_P v_f + k_I\int_0^{T_l} v_f\,ds. \tag{7}$$

The relationship among air enthalpy, temperature and the moisture content leaving the evaporator can be described by:

$$h_s = C_z T_s + h_{fg}W_s. \tag{8}$$

Then, Eqs. (2) and (4) can be rewritten by

$$\rho V\frac{dW_z}{dt} = \rho v_f\left(\frac{h_s-C_z T_s}{h_{fg}}-W_z\right) + M_{load}, \tag{9}$$

$$\rho V_{h2}\frac{dh_s}{dt} = C_z\rho v_f(T_d-T_s) + h_{fg}\rho v_f\left((1-p\%)W_z + p\%W_0-\frac{h_s-C_z T_s}{h_{fg}}\right) + \alpha_2 A_2\left(T_w-\frac{T_d + T_s}{2}\right). \tag{10}$$

The air side convective heat transfer coefficients for the louver finned evaporator under both dry-cooling and wet-cooling regions are calculated as follows [46]:

$$\alpha_1 = j_{e1}\rho v_a\frac{C_z}{Pr^{\frac{2}{3}}},\quad \alpha_2 = j_{e2}\rho v_a\frac{C_z}{Pr^{\frac{2}{3}}}, \tag{11}$$

where Pr is Prandtl number, j_{e1} and j_{e2} are the Colburn factors. The air velocity v_a is described as follows:

$$v_f = dv_a + \varepsilon,$$

where d (m^2) is the cross-sectional area of the conditioned space, ε is the error vector since the air enters or exits through the door or window.

The left-hand side of (1) and (2) is the heat flow into the conditioned space. On the right-hand side of (1), the first term denotes the heat transfer from the DX A/C system to the conditioned space, which is positive if $T_s > T_z$ for the heat mode and negative if $T_s < T_z$ for the cooling mode; the other terms mean the sensible heat load needs to be removed by the DX A/C system. Similarly, on the right-hand side of (2), the first term represents the wet-bulb temperature transferred to the conditioned space, which is positive if $W_s > W_z$ for the humidification mode and negative if $W_s < W_z$ for dehumidification mode; the second term denotes the moisture load to be removed by the DX A/C system. Eqs. (3), (5) and (10) mean that the heat transfer takes place in the inside DX A/C system. In Eq. (3), the first term of the right-hand side represents the heat transfer between the mixed air and the air side at the evaporator; the second term means the heat transfer between the mixed air and the evaporator wall. Eq. (6) represents a dynamic balance of indoor CO_2 concentration.

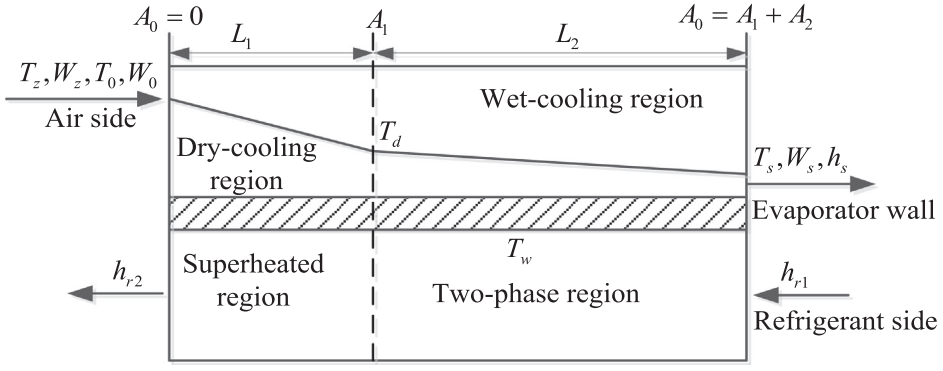

Fig. 2. Simplified diagram of DX evaporator [44].

Remark 1. In this paper, the relationship between the moisture content and temperature at the evaporator outlet [44], $W_s = \frac{0.0198T_s^2 + 0.085T_s + 4.4984}{1000}$, has been released since it may not be feasible under different operating conditions. The proportion of outside air entering into the system is not fixed according to the changing environment during the day. In our previous work [42], we used a variable air volume (VAV) ventilation fan with an independent PSA to reduce indoor CO_2 concentration. In this paper, we use the supply fan to drive the PSA with a built-in PI controller. This results in one less independent control input.

2.3. Load models

Thermal comfort and IAQ are influenced by a set of disturbances, such as external air, solar radiation through opaque and transparent surfaces and internal heat gains due to appliances, lights, occupants, etc. Therefore, good performance for controlling indoor air temperature, humidity and CO_2 concentration is required to deal with the disturbances. When the disturbances are neglected, a large error occurs. Nevertheless, a perfect prediction of disturbances in the future is inadequate in practice. Some disturbances can be measured, such as outside temperature, humidity and CO_2 concentration, and others, such as solar radiation and internal gains, cannot but may be estimated. Next, we will provide more details on the sensible heat load Q_{load}, moisture load M_{load}, pollutant load C_{load}.

The indoor sensible heat load is usually related to the internal loads, including occupants, lighting, equipment, fresh air entering inside and applications and the external loads, including heat transfer conduction through the building walls, roof, floor, doors and heat transfer by radiation through fenestration such as windows and skylights. In this paper, we consider the external load including heat loads by radiation through windows and the fresh air by ventilation. The moisture load is relevant to occupants, equipment, fresh air entering inside and applications. The CO_2 pollutant load is relevant to occupants' respiration. The sensible heat and moisture loads from lighting, equipment and applications are easy to identify, based on their electrical characteristics; the main uncertainties in identifying the sensible heat load and latent heat loads are from the loads associated with the occupants in the conditioned space. The sensible heat and moisture loads by occupants are determined through the current CO_2 emission. To estimate the sensible heat, moisture and indoor pollutant loads, a method is proposed as follows:

$$Q_{load}(t) = Q_{r,load} + Q_{spl} + \mu C_c + \nu + Q_{air}, \tag{12a}$$

$$M_{load}(t) = \phi C_c + \gamma + M_{air}, \tag{12b}$$

$$C_{load}(t) = G{\cdot}Occp, \tag{12c}$$

where μ and ϕ are the sensible heat and moisture gain coefficients, respectively, ν and γ are the certainties sensible heat and moisture loads, respectively. The heat gain of the supply fan Q_{spl} increases with the air volumetric flow rate of supply air as follows:

$$Q_{spl} = k_{spl} v_f. \tag{13}$$

The external heat load by radiation $Q_{r,load}$ through windows is described by the following equation:

$$Q_{r,load} = n_{win}\varepsilon_{win}A_{win}Q_{rad}, \tag{14}$$

where n_{win} denotes whether the conditioned space has a window, i.e., when $n_{win} = 1$, if it has a window, while if $n_{win} = 0$, it does not. The fresh air of the sensible heat load Q_{air} and the moisture load M_{air} in conditioned space are expressed as follows:

$$Q_{air} = p\%C_z\rho v_f(T_0 - T_z), \tag{15a}$$

$$M_{air} = p\%\rho v_f(W_0 - W_z). \tag{15b}$$

Remark 2. In this section, a simple method is given to estimate the indoor sensible heat and moisture loads, and CO_2 pollutant load. An alternative method to estimate cooling load has been reported in [26]. Besides, the weather forecast data from the weather station in Cape Town are qualified for this research, because: (1) the current weather station is precisely predicted and (2) the weather conditions and solar radiation in this area are relatively stable, indicating that the profiles of the predicted outside temperature, relative humidity and CO_2 concentration are representative.

2.4. PMV index

The PMV index is used as a human thermal comfort requirement indicator. This indicator was first proposed by Fanger [47] to predict the average vote of a large group of persons on the thermal sensation scale. This sensation is expressed by relating the integer range $[-3, +3]$ to the qualitative words cold, cool, slightly cool, neutral, slightly warm, warm, and hot. PMV is defined by six variables, namely metabolic rate M (W/m^2), clothing insulating I_{cl} (m^2°C/W), air temperature T_z, air humidity H_z, air velocity v_a (m/s), and mean radiant temperature T_r. The PMV index can be described by the following equation [47]:

$$\begin{aligned} PMV = {} & (0.303e^{-0.036M} + 0.028)\{(M-W) - 3.05\times10^{-3}[5733 - 6.99(M-W) \\ & - P_a] - 0.42[(M-W) - 58.15] - 1.7\times10^{-5}M(5867 - P_a) \\ & - 0.0014M(34 - T_z) - 3.96\times10^{-8}f_{cl}[(T_{cl}+273)^4 - (T_r+273)^4] \\ & - f_{cl}h_c{\cdot}(T_{cl} - T_z)\}, \end{aligned} \tag{16}$$

where W (W/m^2) is the external work; P_a is the partial water vapor pressure in Pascal. The surface temperature of clothing T_{cl} is given by:

$$\begin{aligned} T_{cl} = {} & 35.7 - 0.028(M-W) - I_{cl}\{3.96\times10^{-8}f_{cl}[(T_{cl}+273)^4 - (T_r+273)^4] \\ & + f_{cl}h_c(T_{cl} - T_z)\}, \end{aligned} \tag{17}$$

and the convective heat transfer coefficient h_c is defined as:

$$h_c = \begin{cases} h_c^*, & \text{if } h_c^* > 12.1\sqrt{v_a}, \\ 12.1\sqrt{v_a}, & \text{if } h_c^* < 12.1\sqrt{v_a}, \end{cases} \tag{18}$$

where $h_c^* = 2.38{\cdot}(T_{cl} - T_z)^{0.25}$ is the ratio of body surface area covered by clothes to the naked surface area, can be defined as:

$$f_{cl} = \begin{cases} 1.00 + 1.290I_{cl} & \text{if } I_{cl} \leqslant 0.078, \\ 1.05 + 0.645I_{cl} & \text{if } I_{cl} > 0.078. \end{cases} \tag{19}$$

The mean radiant temperature T_r is determined as [48]:

$$T_r = \left[(T_g + 273)^4 + \frac{1.10\times10^8 v_a^{0.6}}{\epsilon D^{0.4}}(T_g - T_z)\right]^{1/4} - 273, \tag{20}$$

where T_g is the globe temperature; D and ϵ are the globe diameter in meters and the globe emissivity coefficient, respectively. P_a is related to the relative humidity of the air H_z by means of Antoine's equation [49]:

$$P_a = 10H_z e^{(16.6536 - 4030.183/(T_z+235))}, \tag{21}$$

where $H_z = 100W_z/A_{conv}$, A_{conv} is the unit transfer coefficient. The metabolic rate M is determined by [50]:

$$M = \lambda G,$$

where the coefficient λ is a constant. Then the metabolic rate M under a steady state of the indoor CO_2 concentration can be rewritten as follows:

$$M = \frac{\lambda}{Occp}\left(k_P v_f + k_I \int_0^{T_I} v_f\, ds\right)(C_c - C_s).$$

The PMV can be written as a function of the following variables:

$$\text{PMV} = g(T_z, W_z, C_c, v_f, T_r, I_{cl}, T_{cl}). \tag{22}$$

Remark 3. There are several existing metrics to measure human (dis)

comfort, e.g., temperature constraint violations [26], comfort penalty [17], predicted percentage dissatisfied (PPD) [51], and PMV index [23,29]. The PMV index has been used as an indicator to maintain indoor comfort temperature [23] and to control indoor temperature and humidity [29]. In this paper, the Eq. (22) implies that the modified PMV index can estimate not only the indoor thermal comfort but also IAQ under a steady state of the indoor CO_2 concentration and keep them in a certain range. This is subjective and can be considered as perfect when PMV = 0.

2.5. Energy models for the DX A/C system

The DX A/C system components that consume energy include the power input of the evaporator fan, compressor fan, and condenser. The power to drive the dampers is assumed to be negligible. The total power consumption P_{tot} of the DX A/C system at time t then is calculated as [52]:

$$P_{tot} = P_e + P_c + P_f, \tag{23}$$

where the fan power input of the evaporator P_e, the fan power of the compressor P_f and the power input of the condenser P_c are given below:

$$P_e = a_0 + a_1 v_f, + a_2 v_f^2 + a_3 T_s + a_4 T_s^2 + a_5 Q_c + a_6 Q_c^2 + a_7 v_f T_s + a_8 v_f Q_c + a_9 T_s Q_c, \tag{24}$$

$$P_f = b_0 + b_1 T_d + b_2 T_s + b_3 T_d^2 + b_4 T_d T_s + b_5 T_s^2 + b_6 T_d^3 + b_7 T_d^2 T_s + b_8 T_d T_s^2 + b_9 T_s^3, \tag{25}$$

$$P_c(t) = c_0 + c_1 m_r + c_2 m_r^2, \tag{26}$$

where the coefficients $a_i (i = 0,1,...,9), b_i (i = 0,1,...,9), c_i (i = 0,1,2)$ are constant and can be determined by curve-fitting of experimental data in [52]. The indoor cooling load Q_c is the summation of the sensible and latent heat loads.

2.6. Constraints

The DX A/C system is subject to thermal comfort, IAQ and operational constraints defined as below.

(C1) $\mathrm{PMV} \in [\underline{\mathrm{PMV}}, \overline{\mathrm{PMV}}]$. The limit of the PMV value means thermal comfort and IAQ are within the required levels for human.

(C2) $T_z \in [\underline{T}_z, \overline{T}_z], W_z \in [\underline{W}_z, \overline{W}_z], C_c \in [\underline{C}_c, \overline{C}_c]$. The indoor air temperature, moisture content and CO_2 concentration are within the required ranges for occupants in the conditioned space.

(C3) $T_s \in [\underline{T}_s, \overline{T}_s], W_s \in [\underline{W}_s, \overline{W}_s]$. The bounds of the supply air temperature and moisture content are constrained because of the physical characteristics of the coils and the air cooling coils inside the evaporator. Besides, the upper bounds $\overline{T}_s$ and $\overline{W}_s$ are less than T_z and W_z, respectively, since the DX A/C system is operating in the cooling mode. The bound of air enthalpy h_s satisfies: $h_s \in [C_z \underline{T}_s + h_{fg} \underline{W}_s, C_z \overline{T}_s + h_{fg} \overline{W}_s]$ due to (8).

(C4) $T_w \leqslant T_d$. The air temperature after the surface of the DX cooling coil cannot be warm.

(C5) $v_f \in [\underline{v}_f, \overline{v}_f], m_r \in [\underline{m}_r, \overline{m}_r]$. The upper bounds of the air volumetric flow rate $\overline{v}_f$ and mass flow rate of refrigerant $\overline{m}_r$ are limited by the physical characteristics of the DX A/C system. The lower bounds $\underline{v}_f > 0$ and $\underline{m}_r > 0$ match minimum operation and ventilation demands.

(C6) $p\% \in [\underline{p}\%, \overline{p}\%)$. The upper and lower bounds limit the ratio of the fresh air entering indoor.

(C7) $T_d \leqslant (1-p\%) T_z + p\% T_0, W_s \leqslant (1-p\%) W_z + p\% W_0$. The mixed temperature and moisture content between the fresh air and return air after the DX dry-cooling region and wet-cooling region can only decrease, respectively.

By collecting the system dynamic Eqs. (1), (3), (5), (6), (9) and (10), we reach the following:

$$\dot{x}(t) = f(x(t), u(t), w(t)), \tag{27}$$

where the *state vector* of the system is denoted by

$$x = [h_s, T_z, T_d, T_w, W_z, C_c]^T,$$

the *control vector* is denoted by

$$u = [v_f, m_r]^T,$$

the *load vector* is denoted by

$$w = [Q_{load}, M_{load}, C_{load}]^T,$$

the *output vector* is denoted by

$$y = [T_z, W_z, C_c]^T.$$

The constraints in (C1)-(C7) are compactly written as

$$x \in \mathbb{X},\ u \in \mathbb{U},\ PMV \in \mathbb{F},\ p \in \mathbb{P},\ T_s \in \mathbb{T}_s,\ W_s \in \mathbb{W}_s, \text{ and } h(x) \leqslant 0, \tag{28}$$

where $\mathbb{X}, \mathbb{U}, \mathbb{P}, \mathbb{T}_s$ and $\mathbb{W}_s$ are bounded sets, and $h(x)$ is a function of state variables.

2.7. TOU Strategy

In this paper, the energy charge is determined based on the TOU strategy. The TOU electricity tariff is a typical program of demand-side management, in which the electricity price changes over different periods based on the electricity supply cost; for example, a high price σ_h for peak periods $\mathscr{T}_h$, medium price σ_m for standard periods $\mathscr{T}_m$ and low price σ_l for off-peak periods $\mathscr{T}_l$. In this study, the daily TOU electricity price can be described as

$$\sigma(l) = \begin{cases} \sigma_h = 0.20538\text{"\$"/kW h}, & l \in \mathscr{T}_h, \\ \sigma_m = 0.05948\text{"\$"/kW h}, & l \in \mathscr{T}_m, \\ \sigma_l = 0.03558\text{"\$"/kW h}, & l \in \mathscr{T}_l, \end{cases} \tag{29}$$

where $\mathscr{T}_h = (8,11] \bigcup (19,21], \mathscr{T}_l = (0,7] \bigcup (23,24]$ and $\mathscr{T}_m = (7,8] \bigcup (11,19] \bigcup (21,23]$. "\$" is the United States dollar and time $\mathscr{T}$ is the whole period of the day with $l = 1,...,24$. Since there is a big difference in energy prices between the peak and off-peak hours, cost savings can be expected if significant amount of peak power consumption is shifted to off-peak hours. To minimize the energy cost, some previous optimization control strategies are reported in [18,25]. In this paper, we propose an alternative optimisation control scheme to minimize not only the energy cost but also the energy consumption.

3. Hierarchical control

Hierarchical control can be interpreted as an attempt to handle complex problems by decomposing them into smaller subproblems and reassembling their solutions in a hierarchical structure. The idea is to establish a hierarchical control structure composed of two layers. The two layers are adopted by using a control schedule, the simplified scheme of which is described in Fig. 3. The main principle of hierarchical control is as follows. At the upper layer, the objective is performed to compute the optimal conditions with respect to a performance index representing an economic and environmental criterion over a long-term scale horizon H_L with a sampling period T_L. At this stage, a detailed, a physical nonlinear model of the system although static is used. At the lower layer, a simple linear dynamic model is used to design an MPC controller, guaranteeing that the target values transmitted from the upper layer are obtained over a short time horizon $h_l = T_L$ with a smaller sampling period $t_l = T_L/n_l$. Fig. 3 implies that the upper layer sends information to the lower layer at the sampling instant $mT_L (m = 0,1,...,\infty)$; meanwhile, the lower layer receives the information as a task, and then completes the task within the sampling intervals

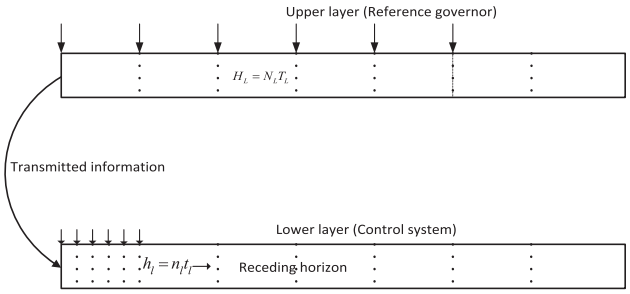

Fig. 3. Simplified schematic of two-layer hierarchical structure scheme.

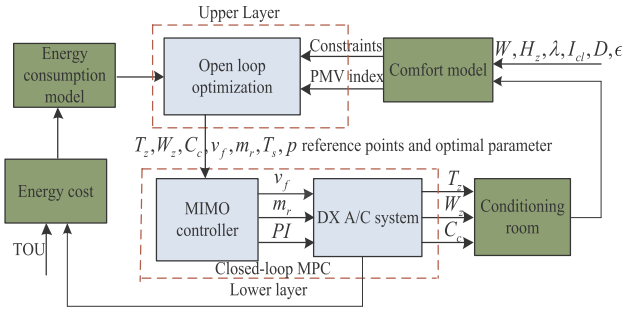

Fig. 4. Conceptual framework of the proposed hierarchical control approach.

$[mT_L + qt_l, mT_L + (q+1)t_l)(q = 0,1,...,n_l-1)$.

This paper presents an autonomous hierarchical control approach to obtain a real-time optimisation scheduling strategy for the DX A/C system to minimise the total energy cost while maintaining the indoor thermal comfort and IAQ within acceptable ranges. The control method is based on a traditional control scheme with a reference governor in the upper layer, named the optimization layer, which, by means of a nonlinear optimizer, is able to generate the steady states and the optimal volume of air entering the system by optimising the energy cost of the DX A/C system and the value of the PMV index under the TOU strategy. Then, the lower layer receives the steady states as input, and the closed-loop MPC controller is designed to track the trajectory references of indoor air temperature, moisture content and CO_2 concentration. The conceptual framework of the proposed autonomous hierarchical control approach is shown in Fig. 4. The details are provided in the following subsections.

3.1. Optimization layer (Upper layer)

At the upper layer, the reference governor has been defined according to the optimization problem described by (30). Note that the PMV index (22) and the energy consumption model (23) are the optimization objectives. At the upper layer, the optimisation problem is considered as an open loop optimal control framework. Considering the DX A/C system (27) and its constraints (28), we formulate the following optimal controller to generate the steady states.

$$\min(\alpha|PMV(t_{m_0})| + (1-\alpha)P_{tot}(t_{m_0})\sigma(t_{m_0})), \tag{30}$$

subject to the following constraints:

$$f(x(t_{m_0}),u(t_{m_0}),T_s(t_{m_0}),p(t_{m_0})) = 0, \tag{31}$$

$$x(t_{m_0}) \in \mathbb{X},\ u(t_{m_0}) \in \mathbb{U},\ PMV(t_{m_0}) \in \mathbb{F},\ p(t_{m_0}) \in \mathbb{P},\ T_s(t_{m_0}) \in \mathbb{T}_s,\ W_s(t_{m_0}) \in \mathbb{W}_s,\ h(x(t_{m_0})) \leqslant 0, \tag{32}$$

where α is a weighting factor ($0 < \alpha < 1$), x,u and $f(\cdot)$ are denoted in (27). $x(t_{m_0}),u(t_{m_0}),v(t_{m_0})$ are the optimization variables for $m = 0,...,N_L-1$, where $v = [p,T_s,T_r,T_{cl}]$.

Assuming that all the variables are within the bounded sets, feasible solutions exist for the optimization problem (30) by using an open loop controller. Among all the feasible solutions, let $x_s(t_{m_0}),u_s(t_{m_0}),v_s(t_{m_0})$ be the optimal solution of optimization problem (30), and $x_s(t_{m_0}) \in \boldsymbol{X}_s, u_s(t_{m_0}) \in \boldsymbol{U}_s, v_s(t_{m_0}) \in \boldsymbol{V}_s$ for $m = 0,...,N_L-1$. $\boldsymbol{X}_s,\boldsymbol{U}_s,\boldsymbol{V}_s$ are the optimal sequence points of the state, input and parameter variables. In this paper, the optimal sequence points are the steady states of Eq. (31).

Remark 4. The weighting factor α is chosen to balance the tradeoff between the two objectives, which are energy cost and comfort levels. Specifically, a relative large α gives better comfort level but worse cost savings. In the case that α is relatively large, more effort is put into optimizing the most comfortable indoor air temperature, humidity and CO_2, which may result in a loss of balancing capacity. The parameter α can be adjusted by utilities to achieve different goals.

The above nonlinear steady state optimization algorithm is provided as below.

Algorithm 1. Nonlinear Programming algorithm to the DX A/C system static optimization problem.

Initialization: Given initial state values $x(0)$ and $u(0)$. The initial state values are selected within their bounds.

1: Input the data of the outside temperature, relative humidity, sensible heat load, latent heat load and pollutant load.

2: The objective function (30) and constraints in (31) and (32) are converted into the following standard nonlinear programming so that it can be conveniently solved by the Matlab built-in function *fmincon*:

$$\min f_c^T \cdot z \ s.\ t. \begin{cases} c(z) \leqslant 0 \\ ceq(z) = 0 \\ A \cdot z \leqslant b \\ A_{eq} \cdot z = beq \\ lb \leqslant z \leqslant ub \end{cases} \tag{33}$$

3: Solve the above procedure (33).

3.2. Control layer (Lower layer)

As discussed above, for each every sample period T_L, the upper layer controller computes the optimal steady state point and delivers it into the lower layer. The task of the lower layer receives the steady state as the trajectory reference and includes a control algorithm trying to drive the system to track the trajectory reference. Therefore, in this case, this layer consists of a discrete-time MPC controller with a sampling time of $t_{m_q} \in [mT_L + qt_l, MT_L + (q+1)t_l), m = 0,1,...,N_L-1, q = 0,1,...,t_l-1$, which is designed to track the reference point of indoor air temperature, moisture content and CO_2 concentration.

In the sequel, we make a commensurate quantization assumption: all variables are quantised in the two sampling schemes, i.e., they are represented by the starting values and remain these values in the same sampling interval, and the objective functions $PMV(t)$,$P_{tot}(t)$, the TOU function $\sigma(t)$, and the constraints in (C1)-(C7) are coarsely quantised, i.e., they take their corresponding values at mT_L, for all $t \in [mT_L,(m+1)T_L)$. This assumption ensures that if the steady state $(x_s(t_{m_q}),u_s(t_{m_q}))$ would be obtained from the optimisation (30)–(32), then one would have $(x_s(t_{m_q}),u_s(t_{m_q})) = (x_s(t_{m_0}),u_s(t_{m_0}))$.

The lower layer receives the reference points of state vector and input vector, which are defined as $x_s(t_{m_q}) \triangleq [h_{s,s}(t_{m_q}),T_{z,s}(t_{m_q}),T_{d,s}(t_{m_q}),T_{w,s}(t_{m_q}),W_{z,s}(t_{m_q}),C_{c,s}(t_{m_q})]^T$ and $u_s(t_{m_q}) = [v_{f,s}(t_{m_q}),m_{r,s}(t_{m_q})]^T$. Define $\delta T_z(t_{m_q}) = T_z(t_{m_q}) - T_{z,s}$

$$(t_{m_q}),\delta W_z(t_{m_q}) = W_z(t_{m_q})-W_{z,s}(t_{m_q}),\delta C_c(t_{m_q}) = C_c(t_{m_q})-C_{c,s}(t_{m_q}),\delta h_s(t_{m_q}),$$
$$= h_s(t_{m_q})-h_{s,s}(t_{m_q}),\delta T_d(t_{m_q}) = T_d(t_{m_q})-T_{d,s}(t_{m_q}),\delta T_w(t_{m_q})$$
$$= T_w(t_{m_q})-T_{w,s}(t_{m_q}),\delta v_f(t_{m_q}) = v_f(t_{m_q})-v_{f,s}(t_{m_q}),\delta m_r(t_{m_q})$$
$$= m_r(t_{m_q})-m_{r,s}(t_{m_q})$$

as the deviations of states and inputs from their trajectory references at sampling period $[mT_L + qt_l,mT_L + (q + 1)t_l)$. Therefore, the dynamical mathematical equation of the DX A/C system at time t_{m_q} can be linearized and written in a linear state-space representation:

$$\begin{cases}\delta\dot{x}(t_{m_q}) = A_c(x_s(t_{m_0}),u_s(t_{m_0}))\delta x(t_{m_q}) + B_c(x_s(t_{m_0}),u_s(t_{m_0}))\delta u(t_{m_q}),\\ y(t_{m_q}) = C\delta x(t_{m_q}) + y_s(t_{m_0}),\end{cases} \tag{34}$$

where the state variables $\delta x(t_{m_q}) = x(t_{m_q})-x_s(t_{m_0}) = [\delta h_s(t_{m_q}),\delta T_z(t_{m_q}),\delta T_d(t_{m_q}),\delta T_w(t_{m_q}),\delta W_z(t_{m_q}),\delta C_c(t_{m_q})]^T$, the input variables $\delta u(t_{m_q}) = u(t_{m_q})-u_s(t_{m_q}) = [\delta v_f(t_{m_q}),\delta m_r(t_{m_q})]^T$,$y_s(t_{m_0}) = [T_{z,s}(t_{m_0}),W_z(t_{m_0}),C_{c,s}(t_{m_0})]^T$ and $y(t_{m_q}) = [T_z(t_{m_q}),W_{z,s}(t_{m_q}),C_c(t_{m_q})]^T$ are the original output variables.

$A(x_s(t_{m_0}),u_s(t_{m_0})),B(x_s(t_{m_0}),u_s(t_{m_0})),C$ are the system state matrix, input matrix and output matrix at the sampling time t_{m_q}, respectively, which can be calculated by:

$$A_c(x_s(t_{m_0}),u_s(t_{m_0})) = \frac{\partial f(x(t_{m_0}),u(t_{m_0}))}{\partial x(t_{m_0})}\Big|_{\substack{x(t_{m_0})=x_s(t_{m_0}),\\ u(t_{m_0})=u_s(t_{m_0})}}$$

$$B_c(x_s(t_{m_0}),u_s(t_{m_0})) = \frac{\partial f(x(t_{m_0}),u(t_{m_0}))}{\partial u(t_{m_0})}\Big|_{\substack{x(t_{m_0})=x_s(t_{m_0}),\\ u(t_{m_0})=u_s(t_{m_0})}}$$

and

$$C = \begin{bmatrix}0 & 1 & 0 & 0 & 0 & 0\\ 0 & 0 & 0 & 0 & 1 & 0\\ 0 & 0 & 0 & 0 & 0 & 1\end{bmatrix}.$$

Consider the discrete-time version of (34):

$$\begin{cases}\delta x(t_{m_{q+1}}) = A_d(x_s(t_{m_0}),u_s(t_{m_0}))\delta x(t_{m_q}) + B_d(x_s(t_{m_0}),u_s(t_{m_0}))\delta u(t_{m_q}),\\ y(t_{m_q}) = C\delta x(t_{m_q}) + y_s(t_{m_0}),\end{cases} \tag{35}$$

where $x(t_{m_q}),u(t_{m_q})$ and $y(t_{m_q})$ are the state vector, input vector and output vector at sampling instant $mT_L + qt_l,m = 0,1,...,N_L-1,q = 0,1,...,n_l-1$.

$A_d(x_s(t_{m_0}),u_s(t_{m_0})) = e^{A_c(x_s(t_{m_0}),u_s(t_{m_0}))t_l}$,$B_d(x_s(t_{m_0}),u_s(t_{m_0}))$ are the $= (\int_0^{t_l} e^{A_c(x_s(t_{m_0}),u_s(t_{m_0}))\tau}d\tau)B_c(x_s(t_{m_0}),u_s(t_{m_0}))$ system state matrix and input matrix, respectively.

The objective of the proposed MPC controller is to maintain the indoor air temperature, moisture content and CO_2 concentration at the required levels with low energy cost. To achieve this aim, the cost function to be minimised can be chosen as

$$\min_{\delta u} J(t_{m_q}) = \underbrace{\sum_{j=1}^{n_p} \|y(t_{m_{q+j}}|t_{m_q})-r(t_{m_{q+j}})\|^2}_{(a)} + R_{\delta u}\underbrace{\sum_{j=0}^{n_c-1} \|\delta u(t_{m_{q+j}})\|^2}_{(b)}, \tag{36}$$

subject to:

$$\begin{cases}\delta x(t_{m_{l_1}}|t_{m_{q+1}}) = A_d(x_s(t_{m_0}),u_s(t_{m_0}))\delta x(t_{m_{l_1-1}}|t_{m_q})\\ \qquad\qquad + B_d(x_s(t_{m_0}),u_s(t_{m_0}))\delta u(t_{m_{l_1-1}}|t_{m_q}),\\ y(t_{m_{l_1-1}}|t_{m_q}) = C\delta x(t_{m_{l_1-1}}|t_{m_q}) + y_s(t_{m_0}),\end{cases} \tag{37}$$

$$\delta x(t_{m_{l_1}}|t_{m_q}) + x_s(t_{m_0}) \in \mathbb{X},\delta u(t_{m_{l_2}}) + u_s(t_{m_0}) \in \mathbb{U},$$
$$l_1 = q + 1,...,q + n_p,l_2 = q,...,q + n_c-1,$$
$$q = 0,1,...,n_l-1,m = 0,1,...,N_L-1. \tag{38}$$

where (a) penalizes the indoor air temperature, moisture content and CO_2 concentration tracking error and (b) penalizes the balancing signal tracking error in quadratic forms. The current time index t_{m_q} denotes the current time $mT_L + qt_l$;$|t_{m_q}$ means that the predicted value is based on the information up to $t = mT_L + qt_l$;$n_p = T_L/t_l$ is the prediction horizon; $n_c = T_L/t_l$ is the control horizon; $r(t_{m_{q+j}})$ is the reference vector at step $t_{m_{q+j}}$;$y(t_{m_{q+j}}|t_{m_q})$ is the predicted output vector at step $t_{m_{q+j}}$;$\delta u(t_{m_{q+j}})$ is the predicted control vector at step $t_{m_{q+j}}$;$R_{\delta u}$ is used as a tuning parameter for the desired closed-loop performance.

Remark 5. The system matrices of the system (34) are updated to $A_d(x_s(t_{(m+1)_0}),u_s(t_{(m+1)_0}))$ and $B_d(x_s(t_{(m+1)_0}),u_s(t_{(m+1)_0}))$ when the system transiting from the sampling interval $[mT_L + (n_l-1)t_l,(m + 1)T_L)$ to $[(m + 1)T_L,(m + 1)T_L + t_l)$. On the other hand, on sampling interval $[(m + 1)T_L,(m + 1)T_L + t_l)$, the variables $\delta x(t_{m_{n_l-1}})$ and $\delta u(t_{m_{n_l-1}})$ as the initial points are fed to the system (37), and the references are updated in (36). The convergence for this periodic MPC for an optimisation problem over an infinite time horizon has been proven in [53,54].

The proposed MPC algorithm is as below:

Algorithm 2. MPC algorithm to the DX A/C tracking control problem.

Initialization: Given initial state value $x(0)$ and let $t_{m_q} = 0(m = 0,q = 0)$.

1: Compute the optimal solution $\overline{U}(t_{m_0}) = [\overline{u}(t_{m_0}),\overline{u}(t_{m_1}),...,\overline{u}(t_{m_{n_l-1}})]^T$ of the problem formulated in (36) and (38).

2: Apply the MPC control $u_{mpc}(t_{m_0}) = \overline{u}(t_{m_0})$ to the system in the sampling interval $[t_{m_0},t_{m_0} + t_l)$; the rest of the solutions $\overline{u}(t_{m_q}),q = 1,...,n_l-1$ are discarded. $x(t_{m_{q+1}})$ is calculated by $x(t_{m_{q+1}}) = f(x(t_{m_q}),u_{mpc}(t_{m_q}))$.

3: Set $t_{m_q} := t_{m_{q+1}}$, and update system states, inputs and outputs with control $u_{mpc}(t_{m_0})$ and state equation $x(t_{m_{q+1}}) = f(x(t_{m_q}),u_{mpc}(t_{m_q}))$.

4: Until $t_{m_q} := t_{m_{n_l-1}}$, and update system states, inputs and outputs; repeat the steps 1 and 2, we have obtain that $u_{mpc}(t_{m_{n_l-1}}) = \overline{u}(t_{m_{n_l-1}})$. Apply the MPC control $u_{mpc}(t_{m_{n_l-1}})$ to the system in the sampling interval $[t_{m_{n_l-1}},t_{(m+1)_0})$.

5: Set $t_{m_q} := t_{(m+1)_0}$, measure the state value $x(t_{m_{n_l-1}})$ by the step $t_{m_q} = t_{m_{n_l-1}}$, and $u_{mpc}(t_{m_{n_l-1}})$ to the system $x(t_{(m+1)_0}) = f(x(t_{m_{n_l-1}}),u_{mpc}(t_{m_{n_l-1}}))$, and update reference $r(t_{m_0}) := r(t_{(m+1)_0})$ in (36).

6: Compute the optimal solution $\overline{U}(t_{(m+1)_0}) = [\overline{u}(t_{(m+1)_0}),\overline{u}(t_{(m+1)_1}),...,\overline{u}(t_{(m+1)_{n_l-1}})]^T$ of the problem formulated in (36) and (38). Then the MPC control $u_{mpc}(t_{(m+1)_0}) = \overline{u}(t_{(m+1)_0})$ (the remaining $\overline{u}(t_{(m+1)_q}),q = 1,...,n_l-1$ are discarded) is applied to the system in the sampling interval $[t_{(m+1)_0},t_{(m+1)_0} + t_l)$ to obtain the closed-loop MPC solution $x(t_{(m+1)_1}) = f(x(t_{(m+1)_0}),u_{mpc}(t_{(m+1)_0}))$ over the period $[t_{(m+1)_0} + t_l,t_{(m+1)_0} + 2t_l)$.

7: Set $t_{m_q} := t_{(m+1)_1}$ and go to step 1.

Generally, the above MPC algorithm never stops, and it updates the controller at each time interval $[t_{m_q},t_{m_{q+1}})$ to include feedback information.

4. Results

Here, a case study is presented to demonstrate the performance of the closed-loop system with the proposed hierarchical control for the DX A/C system. The proposed hierarchical control strategy is compared with a baseline strategy through simulations over a 24-h period.

4.1. System setup

In the case study, an office room is taken as the conditioned space. The volume of the DX conditioned space is 77 m^3. The parameters of the DX A/C system are listed in Table 1. For the proposed hierarchical control strategy, the values of the system dynamic variable constraints are listed in Table 2, and we constrain the value of the PMV in the range of [−0.5,0.5] to ensure that the DX A/C system is able to control indoor thermal comfort and IAQ at acceptable levels. The coefficients of the energy consumption models (23) of the DX A/C system are taken from [52], which are summarized in Table 3.

In this paper, data of the outside temperature and relative humidity in a single summer are given, as shown in Fig. 5(a). The data is obtained from a meteorological station located in Cape Town, South Africa. The predicted solar radiative heat flux density profile of Cape Town is shown in Fig. 5(b). The certainty internal sensible and latent heat loads, the external sensible heat load and pollutant load in the conditioned space are predicted in Fig. 6. The values in Figs. 5 and 6 at every hour are commensurately quantised. It is assumed that the PI controller can absorb the CO_2 concentration in the air supply, where $C_s = 360$ ppm is used in this paper.

The TOU schedule for summer hours is summarized in (29); for simplicity, only the TOU energy charge is used in the cost function. The unit of Relative Humidity (RH) is percent (%). $\frac{11.35}{1000}$ kg/kg of moisture content is equivalent to 60% RH in the conditioned space. In addition, the original nonlinear system (27) is used as the system to be controlled in the simulation.

4.2. Two scheduling strategies

Here, we consider two strategies to schedule the operation of the DX A/C system in the conditioned space. One is energy optimised open loop controller and the closed-loop regulation of the MIMO MPC approach, which serves as a baseline strategy [42], and the other is the proposed energy and comfort optimised open loop controller and the closed-loop tracking of the MIMO MPC strategy. To simplify the comparison, the predicted load profiles are the same in both control strategies.

(1) Baseline: The baseline can be described as follows: We first select a setpoint for indoor air temperature and relative humidity based on a comfort zone within the psychrometric chart and a setpoint for CO_2 concentration based on the required level of occupants. The ASHRAE comfort zone is shown in [55]. Its details are omitted here because of space limitations. Under the given setpoint, we can obtain a unique steady state of the DX A/C system by solving the Eqs. (1), (3), (5), (6), (9) and (10) at every hour over a 24-h period. The nonlinear model is then linearised around its steady state. An MPC is designed for the linearised model. The proposed MPC with sampling period 2 min is applied to achieve better performance on thermal comfort and IAQ with superior energy efficiency simultaneously.

(2) Proposed method: For the proposed control strategy, the details are also given as below: We first consider the open loop controller to solve the optimization problem (30) to obtain steady states at every hour. The open loop controller and closed-loop MPC are employed to track the references of temperature, humidity and CO_2 concentration. In the proposed control method, the volume of the outside air entering indoor is optimized. The optimal volume of the outside air is used in the DX A/C system for closed-loop MPC controller. The sampling period is set to $T_L = 1$ h; the sampling interval is set to $N_L = 24$ hour; the sampling period for MPC design is $t_l = 2$ min, the prediction horizon and control horizon are taken as $n_p = n_c = 30$ in the lower layer. At each time step, the open loop controller is employed to solve the optimization problem (30) and the steady states obtained are sent to the lower layer. In Section 4.3, we will compare the energy consumption and energy cost for the baseline and the proposed strategies next.

Table 1
Parameters of system model.

Notations	Values	Notations	Values
ρ	1.2 kg/m^3	h_{fg}	2450 kJ/kg
V	77 m^3	ε_{win}	0.45
V_{h1}	0.04 m^3	V_{h2}	0.16 m^3
k_{spl}	0.0251 kJ/m^3	C_z	1.005 kJ kg^{-1} $°C^{-1}$
A_0	22.07m^2		

Table 2
Constraints of system variables.

Notations	Values	Notations	Values
$\overline{T}_s$	22 °C	$\underline{T}_s$	8 °C
$\overline{T}_z$	26 °C	$\underline{T}_z$	22 °C
$\overline{T}_d$	22 °C	$\underline{T}_d$	10 °C
$\overline{T}_w$	22 °C	$\underline{T}_w$	10 °C
$\overline{W}_z$	12.3/1000 kg/kg	$\underline{W}_z$	9.85/1000 kg/kg
$\overline{C}_c$	800×10^{-6} ppm	$\underline{C}_c$	650×10^{-6} ppm
$\overline{W}_s$	9.85/1000 kg/kg	$\underline{W}_s$	7.85/1000 kg/kg
$\overline{h}_s$	46.3 kJ/kg	$\underline{h}_s$	27.3 kJ/kg
$\overline{v}_f$	0.8 m^3/s	$\underline{v}_f$	0 m^3/s
$\overline{m}_r$	0.11 kg/s	$\underline{m}_r$	0 kg/s

Table 3
Coefficients of energy consumption models.

Notations	Values	Notations	Values
a_0	900.5	a_1	−8.1
a_2	6.18	a_3	−0.15
a_4	−4.61	a_5	0.02
a_6	−0.2	a_7	0.01
a_8	0.12	a_9	0.09
b_0	−6942	b_1	82
b_2	−0.7	b_3	2.4
b_4	−2.5	b_5	2.68
b_6	0.03	b_7	−0.02
b_8	0.04	b_9	0.0001
c_0	138.1	c_1	0.52
c_2	−2.3		

4.3. Comparison of two strategies

The performance of both strategies is compared with historical weather data of a specific day in Cape Town. The total simulation time is $K = 24$ h. The predicted indoor cooling loads profile is depicted in Fig. 7 overlaid with an electricity rate for summer hours. We duplicate the indoor cooling loads profile for the next day to simulate the MPC scheme. The temperature profile of the air leaving the DX evaporator and p% of the outside air entering into the system over a 24-h period are shown in Fig. 8(a) and (b). The data is used in the DX A/C system for closed-loop tracking control.

The controls computed from two strategies are applied to the DX A/C system. The tracking reference points of indoor air temperature in the conditioned space for the proposed strategy and the setpoint regulation of indoor air temperature for the baseline strategy are depicted in Fig. 9(a). The tracking reference points of indoor air relative humidity in the conditioned space for the proposed strategy and the setpoint regulation of indoor air relative humidity for the baseline strategy are depicted in Fig. 9(b). The tracking reference points of indoor CO_2 concentration in the conditioned space for the proposed strategy and the setpoint regulation of indoor CO_2 concentration for the baseline strategy are depicted in Fig. 9(c). We observe that the indoor temperature, humidity and CO_2 concentration for the proposed strategy can track their reference points well. We also observe that for the proposed

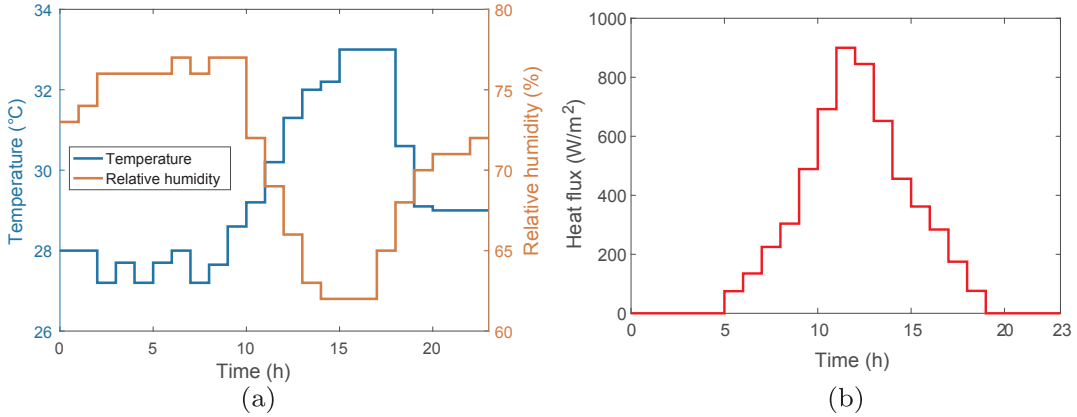

Fig. 5. (a) Profiles of outside temperature and relative humidity over a 24-h period. (b) Profiles of radiative heat flux over a 24-h period.

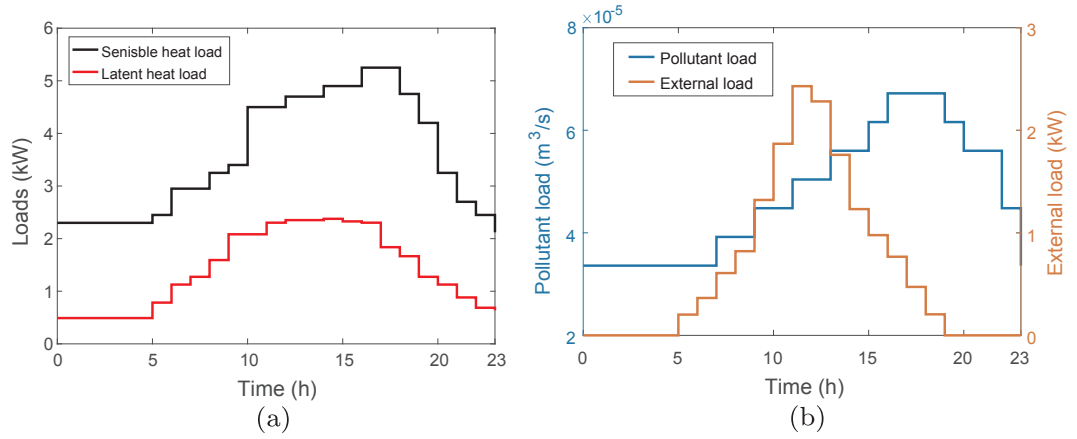

Fig. 6. (a) Certainty internal sensible and latent heat loads. (b) pollutant load and external sensible heat load.

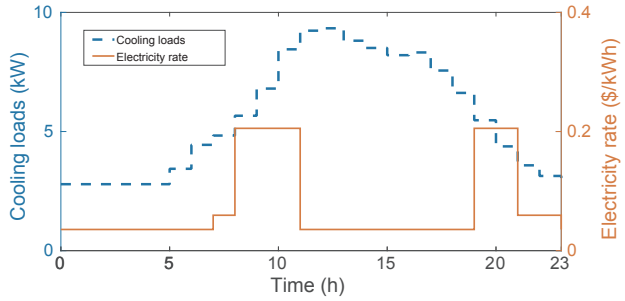

Fig. 7. Cooling loads and electricity rates over a 24-h period.

strategy the reference points are tallish during peak hours for temperature and humidity tracking. This is because the proposed controller can automatically adjust the reference points upward during peak hours such that the energy cost and energy consumption are minimized while both the thermal comfort and IAQ still maintain in the acceptable ranges. We further observe that with the baseline strategy under the varying loads, the MPC controller always maintains the indoor temperature, humidity and CO_2 concentration at their setpoint by regulating the control inputs. From the local zooming out of Fig. 9, the reference points of indoor air temperature, humidity and CO_2 concentration are reached after a transient process of 18 min. After reaching their reference points, the proposed controller maintains the

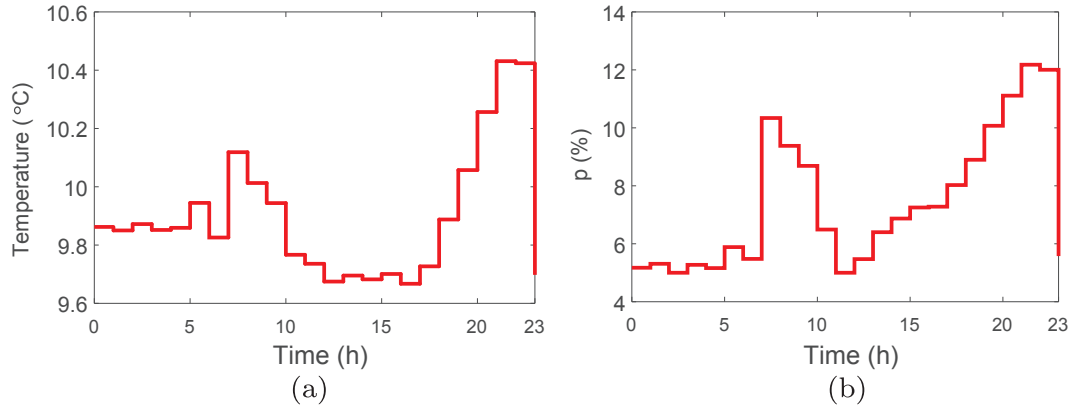

Fig. 8. (a) Supply air temperature over a 24-h period. (b) p% of fresh air entering into the system over a 24-h period.

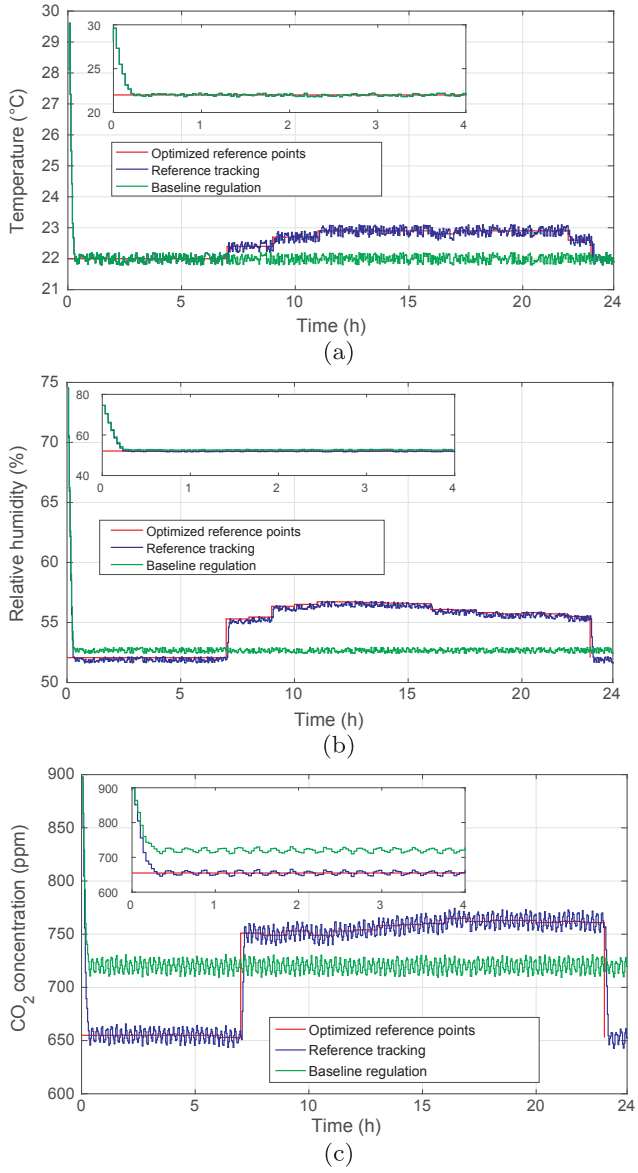

Fig. 9. (a) Temperature tracking. (b) Relative humidity tracking. (c) CO_2 concentration tracking.

reference points with small variation ranges. Fig. 10 shows the air volumetric flow rate and mass flow rate of refrigerant over a 24-h period. The two input variables vary to drive the indoor air temperature,

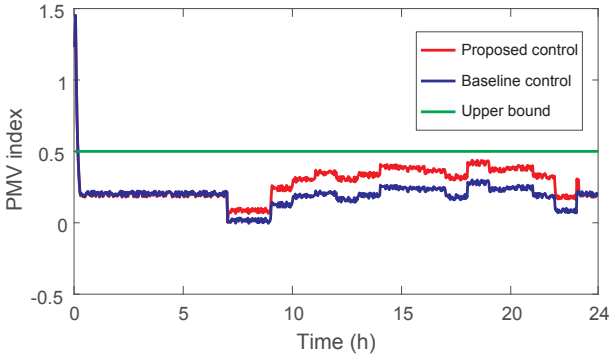

Fig. 11. Profile of the value of the PMV index over a 24-h period.

humidity and CO_2 concentration to track their trajectory references according to the changing environment during the day. In Fig. 11, it can be observed that the values of the PMV index for the two control methods lie within the expected range $[-0.5,0.5]$.

Fig. 12(a) and (b) illustrate the energy consumption and cost of the DX A/C system operation for the proposed strategy and the baseline strategy. We observe from Fig. 12(a) and (b) that both strategies consume almost the same energy cost from 0:00 to 7:00. The indoor temperature, humidity and CO_2 concentration reference points stay at the lower bound of the PMV index during off-peak hours without more cost. After 8:00, the energy costs of the baseline and proposed strategies start to increase since the increased cooling loads are required to be removed and the electric power price is increased. Compared to the baseline strategy, Fig. 12(a) shows that the proposed method consumes less energy. Comparing the two strategies, we observe that under the proposed method, more energy costs are reduced during peak hours. The reason is that the proposed method automatically adjusts upward the reference points such that the energy consumption and the energy costs are minimized during peak hours while maintaining both thermal comfort and IAQ at the required levels. From the simulation, it is verified that the major energy consumption and costs have been reduced effectively during peak hours. We summarize the total energy consumption, energy cost and comfort levels in Table 4. According to it, the proposed hierarchical control strategy performs better than the baseline by around 31.38% in terms of total energy consumption, and by around 33.85% in terms of total energy cost. It can be seen from Table 4 that the proposed control strategy presents a lower energy consumption and costs compared to the baseline control strategy. The table also shows that the total values of the PMV index for the proposed control strategy is higher than that of the baseline control strategy. It is expected that the proposed control strategy reduces energy consumption and cost at the expenses of the comfort level, which is still reasonably and optimally regulated to acceptable levels. Therefore, the utilities can choose

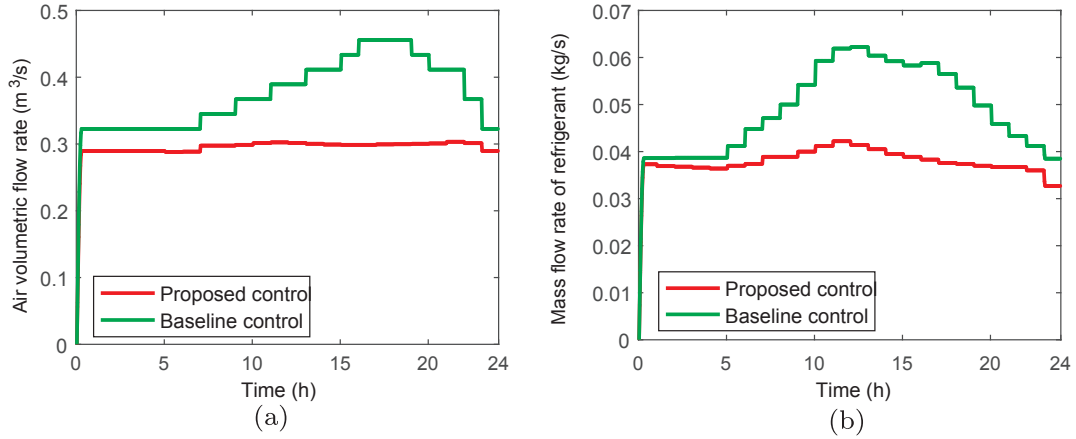

Fig. 10. (a) Air volumetric flow rate over a 24-h period. (b) Mass flow rate of refrigerant over a 24-h period.

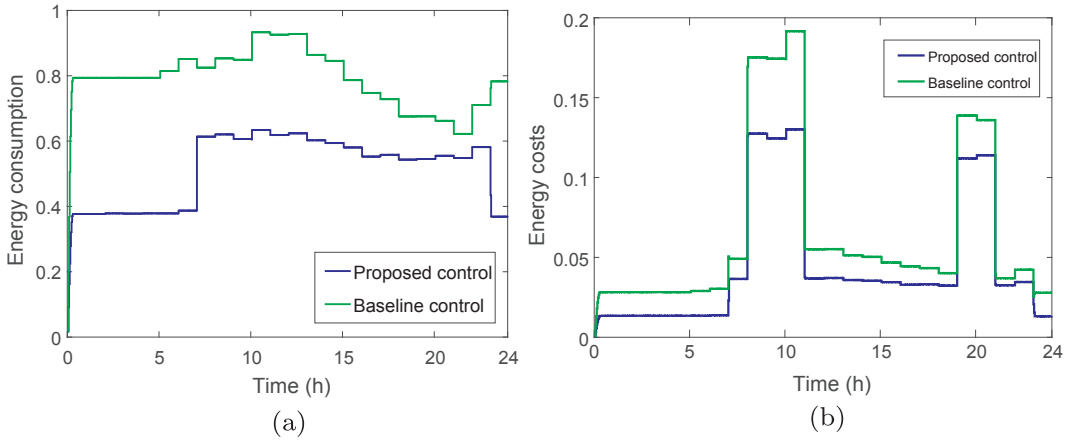

Fig. 12. (a) Energy consumption by two strategies over a 24-h period. (b) Energy cost by two strategies over a 24-h period.

Table 4
Comparison of baseline and proposed strategies.

Control strategy	Energy consumption (kW h)	Energy cost ($)	∑|PMV|
Baseline control	20.52	1.734	103.33
Proposed control	14.08	1.147	162.32
Saving (%)	31.38	33.85	

Table 5
Weather conditions for the testing days.

Date	Control	Average T_0	Average H_0	T_0^{max}	H_0^{max}
12/30	Baseline	28.6	72.4%	33.9	80%
12/31	Proposed	29.2	71.6%	34.2	81%
01/01	Proposed	28.8	72.1%	32.2	79%
01/02	Proposed	28.9	72.4%	33.2	81%
01/03	Proposed	28.1	73.2%	32.0	82%
01/04	Baseline	28.0	72.3%	32.4	79%
01/05	Baseline	27.6	73.4%	32.0	80%

the two control strategies to implement building DX A/C systems based on their different aims.

Though it is desirable to calculate the cost savings brought by the proposed control strategy over the baseline strategy, it is an impossible task for real buildings to simply compare the cost values of two control strategies in one day because load factors and ambient temperature and humidity cannot be the same in every day. To demonstrate the effectiveness of the proposed automatic hierarchical control strategy in different conditions, the proposed testing days happened to be much warmer than the baseline days in this test. The weather conditions of the testing days are shown in Table 5. The energy consumption in the testing days is shown in Fig. 13. From this comparison, all proposed control testing days have much lower power consumption, showing successful energy efficiency improvement by the proposed control strategy.

4.4. Parameter sensitivities analysis

The simulation results presented here are obtained under the assumption that the parameters are accurate and the DX A/C system models can perfectly represent the real system. However, in reality, there usually exist uncertainties in parameters and models. In this section, a simple uncertainty analysis is carried out to demonstrate how the uncertainty parameter would affect the potential performance of the proposed autonomous hierarchical control strategies. Here, we consider the uncertainties of some major parameters of the DX A/C system, namely, the heat transfer area of the DX evaporator in the dry-cooling region A_1 and the heat transfer area of the DX evaporator in the wet-cooling region A_2. The total area $A_0 = A_1 + A_2$ is known. Hence, it is only necessary to consider the effect of the uncertainty parameter A_1 on the performance of the proposed control technique. The open loop optimal controller and the closed-loop tracking of the MPC with different values of the uncertainty parameter A_1 are verified through simulation. For the case study considered here, the simulations for indoor air temperature optimised by open loop optimal controller and the closed-loop MPC temperature tracking under different parameter values are depicted in Figs. 14 and 15, and the results for the open loop optimal controller under all different ranges of the uncertainty parameter

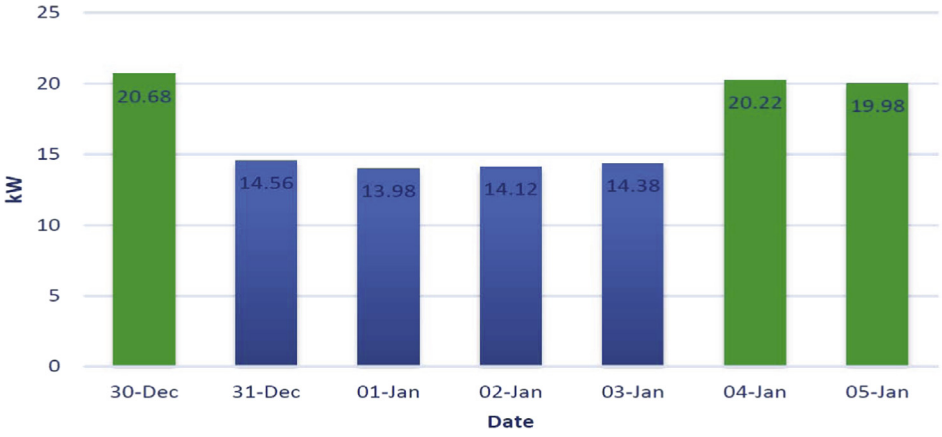

Fig. 13. Energy consumption for the proposed and baseline strategies testing days.

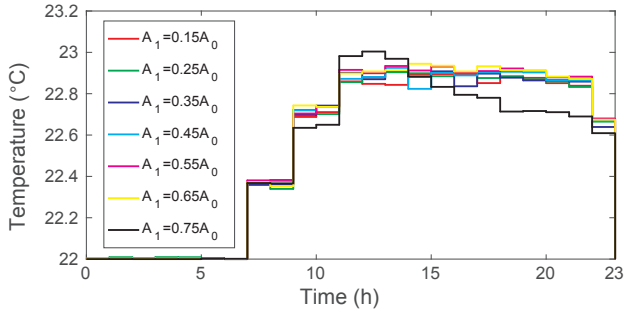

Fig. 14. Steady state of indoor air temperature optimised by the open loop controller under different values of the dry-cooling regions.

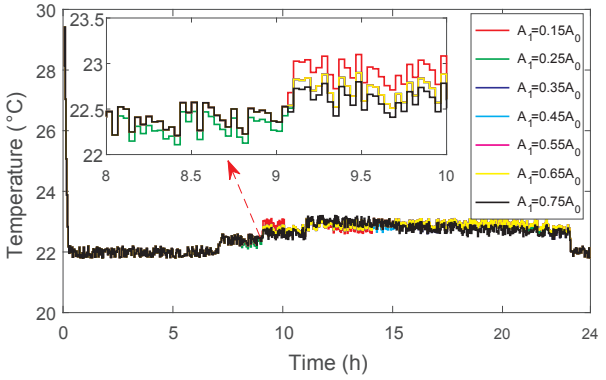

Fig. 15. Closed-loop MPC temperature tracking under different values of the dry-cooling regions.

are listed in Table 6. The standard deviations for the steady state of indoor air temperatures are less than 0.2 °C. The standard deviations for the objective function values of the open loop controller are less than 6%. The results show that the fluctuation of the control performances caused by parameter uncertainty is relatively small. Thus, the proposed autonomous hierarchical control strategy is not very sensitive to the modeling parameter A_1 specified here.

Table 6
Open loop optimization results under different values of the dry-cooling regions.

Objective function value of open loop optimization	Area of dry region	Portion of A_1 m^2	Derivation %
43.04	$(0,0.05A_0]$	$0.05A_0$	2.14%
44.23	$(0.05A_0,0.10A_0]$	$0.10A_0$	0.57%
43. 98	***(0. 1A0,0. 15A0]***	$0.15A_0$	
43.00	$(0.15A_0,0.20A_0]$	$0.20A_0$	2.23%
43.20	$(0.2A_0,0.25A_0]$	$0.25A_0$	1.77%
43.48	$(0.25A_0,0.30A_0]$	$0.30A_0$	1.14%
42.87	$(0.3A_0,0.35A_0]$	$0.35A_0$	2.52%
41.57	$(0.35A_0,0.40A_0]$	$0.40A_0$	5.48%
42.54	$(0.4A_0,0.45A_0]$	$0.45A_0$	3.27%
42.47	$(0.45A_0,0.50A_0]$	$0.50A_0$	3.43%
42.21	$(0.50A_0,0.55A_0]$	$0.55A_0$	4.02%
42.26	$(0.55A_0,0.60A_0]$	$0.65A_0$	3.91%
44.00	$(0.60A_0,0.70A_0]$	$0.70A_0$	0.04%
42.22	$(0.70A_0,0.75A_0]$	$0.75A_0$	4.00%
41.91	$(0.75A_0,0.80A_0]$	$0.80A_0$	4.71%
41.60	$(0.80A_0,0.85A_0]$	$0.85A_0$	5.41%
41.52	$(0.85A_0,0.90A_0]$	$0.90A_0$	5.59%
41.70	$(0.90A_0,0.95A_0]$	$0.95A_0$	5.18%

5. Conclusions

This work formulates an autonomous hierarchical control problem to minimize energy consumption and cost while maintaining both thermal comfort and indoor air quality at the required levels for supervisory control of a direct expansion air conditioning system. It proposes an efficient control algorithm to solve the autonomous hierarchical control problem based on nonlinear programming and closed-loop model predictive control. The optimal reference points of indoor air temperature, humidity and CO_2 concentration for the direct expansion air conditioning system are obtained, and the closed-loop model predictive controller steers the direct expansion air conditioning system to reach the reference points, whereas the energy consumption and energy costs are reduced. Results show that the proposed control method could achieve a reduction of the operation energy consumption by 33.9% and cost by 33.85% with the predicted mean vote value in [-0.5,0.5], respectively. The performances of the proposed control are obtained under the assumption that the models and parameters can perfectly represent the real system. However, in reality, there usually exist uncertainties. The uncertainty analysis has been made in this paper. The results show that the proposed control method is effective because the standard deviations of energy savings are less than 5% in comparison with around 35% energy saving for normal values. The proposed control method is significant to be applied in theoretical and practical applications.

Acknowledgement

The first author would like to express my sincere appreciation to Dr. Xiangguo Xu for his valuable suggestions and academic discussion.

References

[1] Setlhaolo D, Xia X, Zhang J. Optimal scheduling of household appliances for demand response. Electric Pow Syst Res 2014;116:24–8.
[2] Setlhaolo D, Xia X. Optimal scheduling of household appliances with a battery storage system and coordination. Energy Build 2015;94(May):61–70.
[3] Setlhaolo D, Xia X. Combined residential demand side management strategies with coordination and economic analysis. Int J Electric Pow Energy Syst 2016;79:150–60.
[4] Tazvinga H, Xia X, Zhang J. Minimum cost solution of photovoltaic-diesel-battery hybrid power systems for remote consumers. Sol Energy 2013;96:292–9.
[5] Tazvinga H, Zhu B, Xia X. Energy dispatch strategy for a photovoltaic-wind-diesel-battery hybrid power system. Sol Energy 2014;108:412–20.
[6] Tazvinga H, Zhu B, Xia X. Optimal power flow management for distributed energy resources with batteries. Energy Convers Manage 2015;102:104–10.
[7] Zhu B, Tazvinga H, Xia X. Switched model predictive control for energy dispatching of a photovoltaic-diesel-battery hybrid power system. IEEE Trans Control Syst Tech 2015;23:1229–36.
[8] Wu Z, Xia X. Optimal switching renewable energy system for demand side management. Sol Energy 2015;114:278–88.
[9] Wang B, Xia X, Zhang J. A multi-objective optimization model for the life-cycle cost analysis and retrofitting planning of buildings. Energy Build 2014;77:227–35.
[10] Wang B, Xia X. Optimal maintenance planning for building energy efficiency retrofitting from optimization and control system perspectives. Energy Build 2015;96:299–308.
[11] Wu Z, Xia X, Wang B. Improving building energy efficiency by multiobjective neighborhood field optimization. Energy Build 2015;87:45–56.
[12] Wang B, Wu Z, Xia X. A multistate-based control system approach toward optimal maintenance planning. IEEE Trans Control Syst Technol 2017;25(1):374–81.
[13] Wu Z, Wang B, Xia X. Large-scale building energy efficiency retrofit: concept, model and control. Energy 2016;109:456–65.
[14] Fan Y, Xia X. A multi-objective optimization model for energy-efficiency building envelope retrofitting plan with rooftop PV system installation and maintenance. Appl Energy 2017;189:327–35.
[15] Wanjiru EM, Zhang L, Xia X. Model predictive control strategy of energy-water management in urban households. Appl Energy 2016;179:821–31.
[16] Wanjiru EM, Sichilalu SM, Xia X. Model predictive control of heat pump water heater-instantaneous shower powered with integrated renewable-grid energy systems. Appl Energy 2017;204:1333–46.
[17] Morosan P, Bourdais R, Dumur D, Buisson J. Building temperature regulation using a distributed model predictive control. Energy Build 2010;42(9):1445–52.
[18] Ma J, Qin SJ, Salsbury T, Xu P. Demand reduction in building energy systems based on economic model predictive control. Chem Eng Sci 2012;67(1):92–100.
[19] Váňa Z, Cigler J, Široký J, Žáčeková E, Ferkl L. Model-based energy efficient control

applied to an office building. J Process Control 2014;24(6):790–7.
[20] Razmara M, Maasoumy M, Shahbakhti M, Robinett RD. Optimal exergy control of building HVAC system. Appl Energy 2015;156:555–65.
[21] Zhang S, Cheng Y, Fang Z, Huan C, Lin Z. Optimization of room air temperature in stratum-ventilated rooms for both thermal comfort and energy saving. Appl Energy 2017;204:420–31.
[22] Cigler J, Prívara S, Váňa Z, Žáčeková E, Ferkl L. Optimization of predicted mean vote index within model predictive control framework: computationally tractable solution. Energy Build 2012;52:39–49.
[23] Castilla M, Álvarez JD, Normey-Rico JE, Rodríguez F. Thermal comfort control using a non-linear MPC strategy: a real case of study in a bioclimatic building. J Process Control 2014;24(6):703–13.
[24] Castilla M, Álvarez JD, Berenguel M, Rodríguez F, Guzmán JL, Pérez M. A comparison of thermal comfort predictive control strategies. Energy Build 2011;43(10):2737–46.
[25] Ma J, Qin SJ, Salsbury T. Application of economic MPC to the energy and demand minimization of a commercial building. J Process Control 2014;24(8):1282–91.
[26] Ma Y, Matuško J, Borrelli F. Stochastic model predictive control for building HVAC systems: complexity and conservation. IEEE Trans Control Syst Technol 2015;23(1):101–16.
[27] Salsbury T, Mhaskar P, Qin SJ. Predictive control methods to improve energy efficiency and reduce demand in buildings. Comput Chem Eng 2013;51:77–85.
[28] Toftum J, Fanger PO. Air humidity requirements for human comfort. ASHRAE Trans 1999;105:641–7.
[29] Freire R, Oliveira G, Mendes N. Predictive controllers for thermal comfort optimization and energy savings. Energy Build 2008;40(7):1353–65.
[30] Qi Q, Deng S. Multivariable control of indoor air temperature and humidity in a direct expansion (DX) air conditioning (A/C) system. Build Environ 2009;44(8):1659–67.
[31] Xu X, Xia L, Chan M, Deng S. Inherent correlation between the total output cooling capacity and equipment sensible heat ratio of a direct expansion air conditioning system under variable-speed operation (XXG SMD SHR DX AC unit). Appl Therm Eng 2010;30(13):1601–7.
[32] Li N, Xia L, Deng S, Xu X, Chan M. Dynamic modeling and control of a direct expansion air conditioning system using artificial neural network. Appl Energy 2012;91(1):290–300.
[33] Muñoz F, Sanchez EN, Xia Y, Deng S. Real-time neural inverse optimal control for indoor air temperature and humidity in a direct expansion (DX) air conditioning (A/C) system. Int J Refrig 2017;79:196–206.
[34] Yan H, Xia Y, Deng S. Simulation study on a three-evaporator air conditioning system for simultaneous indoor air temperature and humidity control. Appl Energy 2017;207:294–304.
[35] Yan H, Xia Y, Xu X, Deng S. Inherent operational characteristics aided fuzzy logic controller for a variable speed direct expansion air conditioning system for simultaneous indoor air temperature and humidity control. Energy Build 2018;158:558–68.
[36] Zhu Y, Jin X, Fang X, Du Z. Optimal control of combined air conditioning system with variable refrigerant flow and variable air volume for energy saving. Int J Refrig 2014;42:14–25.
[37] Zhu Y, Jin X, Du Z, Fang X, Fan B. Control and energy simulation of variable refrigerant flow air conditioning system combined with outdoor air processing unit. Appl Therm Eng 2014;64:385–95.
[38] Lin SY, Chiu SC, Chen WY. Simple automatic supervisory control system for office building based on energy-saving decoupling indoor comfort control. Energy Build 2015;86:7–15.
[39] Gladyszewska-Fiedoruk K. Correlations of air humidity and carbon dioxide concentration in the kindergarten. Energy Build 2013;62:45–50.
[40] Asif A, Zeeshan M, Jahanzaib M. Indoor temperature, relative humidity and CO_2 levels assessment in academic buildings with different heating, ventilation and air-conditioning systems. Build Environ 2018;133:83–90.
[41] Kim J, Hong T, Jeong J, Lee M, Lee M, Jeong K, et al. Establishment of an optimal occupant behavior considering the energy consumption and indoor environmental quality by region. Appl Energy 2017;204:1431–43.
[42] Mei J, Xia X. Energy-efficient predictive control of indoor thermal comfort and air quality in a direct expansion air conditioning system. Appl Energy 2017;195:439–52.
[43] Yun GY, Choi J, Kim JT. Energy performance of direct expansion air handling unit in office buildings. Energy Build 2014;77:425–31.
[44] Qi Q, Deng S. Multivariable control-oriented modeling of a direct expansion (DX) air conditioning (A/C) system. Int J Refrig 2008;31(5):841–9.
[45] Wang S, Jin X. Model-based optimal control of VAV air-conditioning system using genetic algorithm. Build Environ 2000;35:471–87.
[46] Chen W, Deng S. Development of a dynamic model for a DX VAV air conditioning system. Energy Convers Manage 2006;47(48-49):2900–24.
[47] Fanger PO. Thermal comfort: analysis and applications in environmental engineering. Copenhagen, Denmark: Danish Technical Press; 1972.
[48] Owen MS. 2009 ASHRAE handbook-fundamentals. SI ed. ASHRAE; 2009.
[49] Cena K, Clark J. Bioengineering, thermal physiology and comfort. Studies in environmental science vol. 10. Elsevier Scientific Publishing Company; 1981.
[50] Djongyang N, Tchinda R, Njomo D. Thermal comfort: a review paper. Renew Sustain Energy Rev 2010;14(9):2626–40.
[51] West SR, Ward JK, Wall J. Trial results from a model predictive control and optimisation system for commercial building HVAC. Energy Build 2014;72:271–9.
[52] Vakiloroaya V, Samali B, Pishghadam K. Investigation of energy-efficient strategy for direct expansion air-cooled air conditioning systems. Appl Therm Eng 2014;66(1–2):84–93.
[53] Xia X, Zhang J, Elaiw A. An application of model predictive control to the dynamic economic dispatch of power generation. Control Eng Pract 2011;19:638–48.
[54] Zhang J, Xia X. A model predictive control approach to the periodic implementation of the solutions of the optimal dynamic resource allocation problem. Automatica 2011;47(2):358–62.
[55] ASHRAE. Handbook of HVAC Applications. Atlanta, GA, USA: American Society of Heating, Refrigerating and Air Conditioning Engineers; 2003.